Am J Transl Res 2024;16(8):3582-3598
www.ajtr.org /ISSN:1943-8141/AJTR0157058

Original Article

Diosgenin derivative ML5 attenuates MPTP-induced neuronal impairment via regulating AMPK/PGC-1α-mediated mitochondrial biogenesis and fusion/fission

Jing-Jing Fan*, Wei-Dong Ding*, Ying-Fan Liang, Yao-Xin Wei, Yi Huang, Lei Ma, Rui Wang

*Shanghai Key Laboratory of New Drug Design, School of Pharmacy, East China University of Science and Technology, Shanghai 200237, China. *Equal contributors.*

Received April 7, 2024; Accepted May 14, 2024; Epub August 15, 2024; Published August 30, 2024

Abstract: Objective: The aim of the present study was to assess the therapeutic impact of diosgenin derivative ML5 on Parkinson's disease (PD) and explore the mechanism underlying mitochondrial biogenesis and fusion/fission. Methods: We established 1-methyl-4-phenyl-1,2,3,6-tetrahydropyridine (MPTP)-induced mouse models and N-methyl-4-phenylpyridinium iodide (MPP^+)-induced cell models of PD. The pole test and forced swimming test were used to detect the motor coordination and depressive symptoms in mice. The influence of ML5 on dopaminergic neuronal injury was investigated. Meanwhile, adenosine triphosphate (ATP) content, mitochondrial membrane potential (MMP), and reactive oxygen species (ROS) production were measured to evaluate mitochondrial function. Confocal and transmission electron microscopy were used to detect mitochondrial morphology of cell. The expression of mitochondrial biogenesis-related proteins was measured by Western blotting. Results: The administration of ML5 showed the neuroprotection against MPTP-induced damage *in vivo* and *in vitro*. The levels of ATP, MMP, and ROS were restored after ML5 administration. In addition, we observed that ML5 preserved the mitochondrial network morphology and inhibited mitochondrial fission. Furthermore, the amelioration of mitochondrial dysfunction was mediated by enhancing 5'-monophosphate-activated protein kinase (AMPK) and peroxisome proliferators-activated receptor γ coactivator-l alpha (PGC-1α) expression, which activated its downstream modulators leading to the enhancing of mitochondrial biogenesis and the balance of mitochondrial fusion/fission. Conclusion: ML5 can protect the PD models against MPTP/MPP^+-induced mitochondrial dysfunction and neuronal injury via promoting AMPK/PGC-1α signaling activation and be used as a therapeutic drug for PD treatment.

Keywords: Parkinson's disease, diosgenin derivative, AMPK, mitochondrial biogenesis

Introduction

Parkinson's disease (PD), second only to Alzheimer's disease, is the highest globally prevalent neurodegenerative disease. Dyskinesia is the primary clinical feature of PD, which commonly includes bradykinesia, muscle stiffness, resting tremor, and postural balance disorder, accompanied by other non-motor symptoms [1, 2]. In PD, the substantia nigra (SN) pars compacta of the brain exhibits progressive degeneration or loss of dopaminergic neurons, and accumulation of misfolded alpha-synuclein in Lewy bodies, leading to dopamine shortage within the basal ganglia [3]. In the striatum, dopamine and acetylcholine are two significant neurotransmitters that antagonize and maintain the normal activity of the basal ganglia [4].

Recently, mitochondrial biogenesis has been identified as an essential contributor to neurodegeneration. In addition, it is also critically involved in the maintenance of mitochondrial homeostasis during the mitochondrial life cycle [5]. Meanwhile, mitochondrial biogenesis is significantly mediated by the signaling associated with adenosine 5'-monophosphate-activated protein kinase (AMPK), sirtuin 1 (SIRT1), and peroxisome proliferators-activated receptor γ coactivator alpha (PGC-1α). As an enzyme for phosphorylation at serine/threonine, AMPK can function at AMP/ATP levels during ATP

https://doi.org/10.62347/JBRE5043

depletion and serve as an energy metabolism sensor [6]. The function of histone deacetylase SIRT1, a member of the sirtuin family, depends on coenzyme I. SIRT1 exerts a neuroprotective effect by deacetylating and activating PGC-1α and maintains mitochondrial homeostasis by attenuating the 1-methyl-4-phenyl-1,2,3,6-tetrahydropyridine (MPTP)-caused neurotoxicity [7]. PGC-1α regulates mitochondrial respiration and biogenesis by activating its downstream target genes nuclear factor erythroid 2-related factor 2 (NRF2) and mitochondrial transcription factor A (TFAM). Notably, one of the main AMPK downstream effectors is PGC-1α, whose decreased activity is associated with sporadic PD cases [8]. In neuronal cells, the morphology and migration ability of mitochondria are particularly important. Mitochondria continue to fuse and divide, forming a highly dynamic network structure in cells [9]. It has been discovered that PGC-1α could negatively regulate the expression of dynamin-related protein 1 (Drp1) by binding to its promoter, thereby promote mitochondrial fusion and fission equilibrium [10].

Currently, only symptomatic treatments are available for PD; all these options are associated with adverse effects and cannot stop or delay the advancement of disease. Consequently, the synthesis of multi-targeted drugs is considered an attractive option for the management of neurodegenerative diseases. As a natural steroidal saponin, diosgenin is extracted from *turmeric* or *Dioscorea nipponica* [11]. Researchers have found that diosgenin and its derivatives exert significant pharmacological effects on diseases associated with neurodegeneration, such as PD [12]. Li, et al. [13] found that diosgenin could alleviate movement disorders in PD rats that were induced through injection of lipopolysaccharide into the striatum. In our previous study, we designed and synthesized the multi-target compound ML5 based on the natural product diosgenin, which possesses antioxidant activity. We also introduced the structural fragment of rivastigmine, which has cholinesterase inhibitory activity. ML5 has exhibited a potent antioxidant capacity *in vitro* and neuroprotective activity in rats with bilateral common carotid artery occlusion [14]. In the present study, we further assessed the therapeutic impact of ML5 in MPTP-induced mouse models and MPP^+-induced cell models of PD and explored the mechanism underlying mitochondrial biogenesis and fusion/fission.

Materials and methods

Materials and reagents

The Chinese Academy of Sciences (Shanghai, China) provided SH-SY5Y cells, Gibco (New York, USA) provided trypsin-ethylene diamine tetraacetic acid and fetal bovine serum, and Hyclone (Logan, USA) provided dulbecco's modified eagle medium/ham's F 12 (DMEM/F12) medium. 3-(4,5-dimethylthiazol-2-yl)-2,5-diphenyltetrazolium bromide (MTT), ATP detection reagent kit, bicinchoninic acid protein quantification kit, and mitochondrial membrane potential (MMP) detection kit (JC-1) were obtained from Beyotime Biotechnology Co., Ltd. (Shanghai, China). 2',7'-Dichlorodihydrofluorescein diacetate (DCFH-DA) and MitoTracker Red CMXRos were obtained from Invitrogen (Karlsbad, USA). The antibodies of AMPK, phosphor-AMPK, mitofusin 1/2 (Mfn1/2), optical atrophy 1 (Opa1), Drp1, fission 1 (Fis1), PGC-1α, and tyrosine hydroxylase (TH) were acquired from Cell Signaling Technology (Boston, USA). The antibodies of SIRT1, NRF2, heme oxygenase-1 (HO-1), GAPDH, and Tubulin were purchased from Proteintech (Chicago, USA). The antibodies of choline acetyltransferase (ChAT) and NAD(P)H: quinone oxidoreductase-1 (NQO-1) were purchased from Servicebio (Wuhan, China). MPTP was purchased from Macklin Biological Technology Co., Ltd. (Shanghai, China). MPP^+ was purchased from Yuanye Biotechnology Co., Ltd. (Shanghai, China). The compound ML5 was synthesized by Lei Ma's laboratory at the East China University of Science and Technology (Shanghai, China). Selleck provided the dorsomorphin (compound C) 2HCl (Houston, USA).

Animals and drug administration

The C57BL/6J mice (male, 8 weeks old) were provided by Sipper-BK Experimental Animal (Shanghai, China). The protocols were approved by the Animal Ethics Committee of the East China University of Science and Technology (ethical approval: ECUST-2024-022). We conducted all the animal-related experiments based on the Guide for the Care and Use of Laboratory Animals (National Institutes of Health).

Five groups of ten animals each were created by randomly selecting the control group, model group, 3,4-dihydroxy-L-phenylalanine (L-Dopa) (60 mg/kg) group, ML5 (5 mg/kg) group, and ML5 (20 mg/kg) group. The compound ML5 and L-Dopa (dissolved in saline) were intragastric administered once daily for 15 consecutive days. MPTP (30 mg/kg in saline) was administrated i.p. for 5 days (i.e., days 10-14) in the mice of model, L-Dopa and ML5 groups. Equal volume of saline was used as vehicle control. Then the behavior of the mice was tested on day 15, and the mice were sacrificed on day 16.

Pole test

Based on the study conducted by Xu, et al. [15], the device was designed. The gauze was wrapped around the iron frame to avoid slippage, and a piece of foam board was fixed at a height of 55 cm to prevent mice from climbing. The mice were positioned with their heads straight upward and their tails down at the top of the pole. The locomotion activity time (T-LA) (i.e., when the hind feet of mice left the platform) and the turning time (T-Turn) were recorded. This experiment was conducted thrice for each mouse, and the average values were utilized as the results. The interval between each experiment was ≥15 min. All mouse were trained thrice per day for 3 days to become accustomed to the apparatus prior to the formal experiment.

Forced swimming test

The mice were placed inside a cylindrical water tank with 20 cm deep water at 20-22°C. Next, the immobility time was recorded for the final 4 min during which the mice were allowed to swim for 6 min. There was no training before the formal experiment, and each mouse was only tested once.

Nissl staining

Mice were subjected to transcardial perfusion with saline and 4% paraformaldehyde after asphyxiation of carbon dioxide. The brain was fixed with paraformaldehyde and further embedded in paraffin. Paraffin sections of the SN and striatum (thickness: 4 μm) were analyzed by Servicebio Company (Wuhan, China). Briefly, after dewaxing using xylene and rehydration with gradient alcohol, a 10-minute Nissl staining solution (Beyotime, China) was conducted to stain the sections. After being rinsed with distilled water, sections were dehydrated with different concentrations of ethanol, purified with xylene, and sealed with neutral balsam. Finally, the images were quantified using Image-Pro Plus 6.0 to evaluate the number of positive cells.

Immunohistochemistry

The sections were rehydrated in absolute ethanol, 95% ethanol, 85% ethanol, and distilled water for 5 min after being deparaffinized in xylene (soaked twice for 10 min). Subsequently, an 8-minute heating of the section in citric acid antigen repair solution was conducted using a microwave oven. Following an interval of 7 min, the sections were heated for another 8 min. Thereafter, 20-minute incubation of the sections with hydrogen peroxide (3%) was carried out to remove endogenous peroxidase activity. Then, after blockage of the sections with 5% goat serum and overnight incubation with Antibody I at 4°C, sections were incubated with Antibody II in the humidity chamber for 1 h. Finally, 3,3'-diaminobenzidine was utilized for staining the sections, and the cell nucleus was stained using hematoxylin. For the collected images, the Image-Pro Plus 6.0 software was employed to analyze the images.

Enzyme-linked immunosorbent assay (ELISA)

Appropriate amount of striatal tissue was weighed, ground to homogenate after adding phosphate buffered solution (PBS), centrifuged for 10 min at 4°C, and the supernatant was separated. The levels of dopamine, 3,4-dihydroxyphenylacetic acid (DOPAC), and homovanillic acid (HVA) were examined in the striatum using ELISA kits. After obtaining the optical density values at 450 nm with a microplate reader (BioTek, USA), the relative concentrations were calculated by the standard curve method and expressed as pg/mg.

Cell culture and processing

The DMEM/F12 medium which contained fetal bovine serum (10%), penicillin (100 units/mL), and streptomycin (100 mg/mL) was used to culture SH-SY5Y cells at 37°C with 5% CO_2. The compound ML5 was dissolved in dimethyl sulfoxide and diluted in DMEM/F12 medium to an

indicated final concentration before usage. MPP^+ was diluted to 100 mM with PBS and stored at -20°C. After inoculation and cultivation in 96 or 6-well plates for 24 h, SH-SY5Y cells were processed with ML5 for 2 h as previously described. The serum-free medium was employed to administrate the control and injured cells. Cells in the experimental and injury group were subsequently exposed to MPP^+ (1 mM), which was diluted in a serum-free medium. Equal volume of serum-free medium was given to cells in the control group.

Measurement of cell viability

For the determination of cell viability, we carried out the MTT assay. The 5 mg/mL MTT solution was dissolved in PBS buffer. Following MPP^+ stimulation, each well received MTT solution (10 μL), and then a 4-hour incubation was conducted at 37°C. After discarding the liquid, each well received dimethyl sulfoxide solution (100 μL). Finally, the absorbance at 490 nm was examined by a microplate reader (BioTek, Winooski, USA).

ATP content analysis

The level of ATP was examined using an ATP detection kit. After drug treatment, 200 μL of ATP lysate was given to each well, and 15-minute pre-cold on ice was conducted. After 10-minute centrifugation at 4°C and 12,000 × *g*, the collection of the supernatant was performed. The 96-well whiteboard was filled with ATP detection solution (100 μL) for 3 min in the dark to deplete background ATP. Thereafter, each well received ATP standards or samples (10 μL). After 1 min of the reaction in the dark, the relative light unit value was measured and the standard curve method was applied to calculate the content of ATP.

Evaluation of reactive oxygen species (ROS) levels

ROS levels were detected with the fluorescent vital dye DCFH-DA. This dye is oxidized by ROS to generate DCFH, resulting in fluorescence. Briefly, after 30-minute incubation of the cells with DCFH-DA (10 μM) dissolved in serum-free DMEM/F12 medium at 37°C, a flow cytometer (Beckman Coulter, USA) detection was conducted to examine the fluorescence. Additionally, the cells were also observed and recorded by a fluorescence microscope (Nikon, Tokyo, Japan).

MMP determination

To determine the MMP, we employed a JC-1 fluorescent probe. Along with the elevation of MMP, the accumulated JC-1 probe in the mitochondrial matrix can form a polymer and emit red fluorescence. Conversely, the JC-1 monomer emits green fluorescence. Briefly, after 20-minute incubation of the cells with 1× JC-1 at 37°C in the dark, fluorescence was subsequently determined on a Synergy 2 microplate reader (BioTek, Winooski, USA) at the following wavelengths: red (ex/em = 585/590 nm) and green (ex/em = 514/529 nm). The fluorescence microscope (Nikon, Tokyo, Japan) was used to take representative pictures.

Mitochondrial morphology

A 100 nM concentration of the MitoTracker Red CMXRos was established in a DMEM/F12 serum-free medium. Processed cells were incubated with MitoTracker Red for 15 min avoiding light, and washed thrice with precooled PBS prior to observation. Mitochondrial morphology was observed and recorded by the confocal microscope (Leica, Wetzlar, Germany). The ImageJ software was utilized for image analysis. The form factor (FF) was estimated as follows: $FF = perimeter^2/(4\pi \times area)$.

Transmission electron microscopy (TEM)

Digestion and centrifugation were used to collect the cells. Subsequently, they were transferred into a new TEM fixative for storage and transport at 4°C. After 2-hour fixation of the samples using 1% osmic acid, dehydration using alcohol gradient and purification using 100% acetone were conducted. The samples were permeabilized and embedded in resin, and the ultramicrotome (Leica, Wetzlar, Germany) was used to section the resin blocks into 60-80 nm sections which were fished out onto 150-mesh copper grids. The copper grids were doubly stained with 2% uranium acetate saturated alcohol solution as well as 2.6% lead citrate solution and dried overnight. Observation under TEM (Gatan, California, USA), the images were analyzed using the Image-Pro Plus 6.0 software [16-18].

Western blotting

For western blotting assay, cell lysis and the quantification of proteins were conducted. After separation of the protein samples with a sodium dodecyl sulfate-polyacrylamide gel, transferring the protein bands to 0.45 μm polyvinylidene fluoride membranes (Millipore, USA), and 2-hour blocking of the membrane using 5% skim milk dissolved in tris-buffered saline with 0.2% Tween 20 (TBST) buffer, overnight incubation with Antibody I at 4°C was conducted. After thrice rinsing using TBST, 2-hour incubation of the membranes with Antibody II for 2 h and thrice washing with TBST were carried out. Finally, the membranes were immersed in enhanced chemiluminescence (Yeasen, Shanghai, China) and photographed using the Tannon 5200S chemiluminescence image system (Shanghai, China). The ImageJ software was used to analyze the grey value of the protein.

Statistical analysis

All the values of the results were expressed as mean ± S.E.M. The one-way analysis of variance and LSD post hoc test were applied for the statistical analysis using SPSS 26.0 software (SPSS, Palo Alto, USA). The *P*-value less than 0.05 was set as a significant difference.

Results

ML5 ameliorated MPTP-induced motor dysfunction and alleviated dopaminergic neuronal impairment

ML5 alleviated behavioral deficits in MPTP-induced mouse model of PD: To evaluate the neuroprotective function of ML5 *in vivo*, we established mouse models of PD and carried out follow-up experiments (**Figure 1A**). The structure of compound ML5 is shown in **Figure 1B**. The pole test is typically utilized for assessing the motor coordination and retardation of mice with PD. As shown in **Figure 1C** and **1D**, the T-turn and T-LA required by mice of the model group were more prolonged than those recorded for the control group, indicating that the motor coordination of mice with PD was impaired. Conversely, treatment with L-Dopa and ML5 (5 mg/kg and 20 mg/kg) dramatically shortened the T-turn and total time required by mice with PD, suggesting that motor coordination and retardation were alleviated to some extent. The forced swimming test is commonly utilized for assessing motor competence and depression [19]. The immobility time of the model group was more prolonged than that of the control group. Therapy with L-Dopa, low-dose ML5, and high-dose ML5 significantly reduced the immobility time of mice with PD, indicating improvement in the movement ability and depressive state of mice with PD (**Figure 1E**).

ML5 increased the cell viability in vitro: We sought to examine whether ML5 adversely affected cell viability. Therefore, SH-SY5Y cells were processed with ML5 (0.01, 0.1, and 1 μM) for 24 h. No obvious cytotoxicity of ML5 was observed (**Figure 1F**). As presented in **Figure 1G**, dramatically reduced cell viability was found in the MPP^+-treated model group of cells, but not in control cells, whereas therapies with different doses of compound ML5 markedly increased cell viability.

ML5 promoted neuronal survival in vivo: To further clarify ML5 effect on brain damage in PD mice induced by MPTP, we conducted Nissl staining for the SN and striatum (**Figure 1H-K**). MPTP stimulation significantly decreased the number of Nissl-positive cells in the SN and striatum, and the neurons exhibited shrunken morphology and irregular arrangement. Nevertheless, this effect was counteracted by L-Dopa and ML5 treatment, and the number of neurons in this region was also restored to the normal level. These results indicated that ML5 could decrease MPTP-induced neurotoxicity and exert a significant protective effect on neurons.

ML5 enhanced TH^+ neurons and ChAT expression in SN and striatum of mice with PD: Damage of dopaminergic neurons in SN is considered as a characteristic pathogenic change of PD [20]. TH immunohistochemical staining (**Figure 2A** and **2B**) revealed an abundance and dense arrangement of TH^+ neurons in the SN of the control group. The number of TH^+ neurons in SN was significantly reduced in the model group, and the arrangement of TH^+ neurons was sparse. After treatment with L-Dopa and ML5, the number of neurons in SN was drastically elevated, and the arrangement of TH^+ neurons was improved.

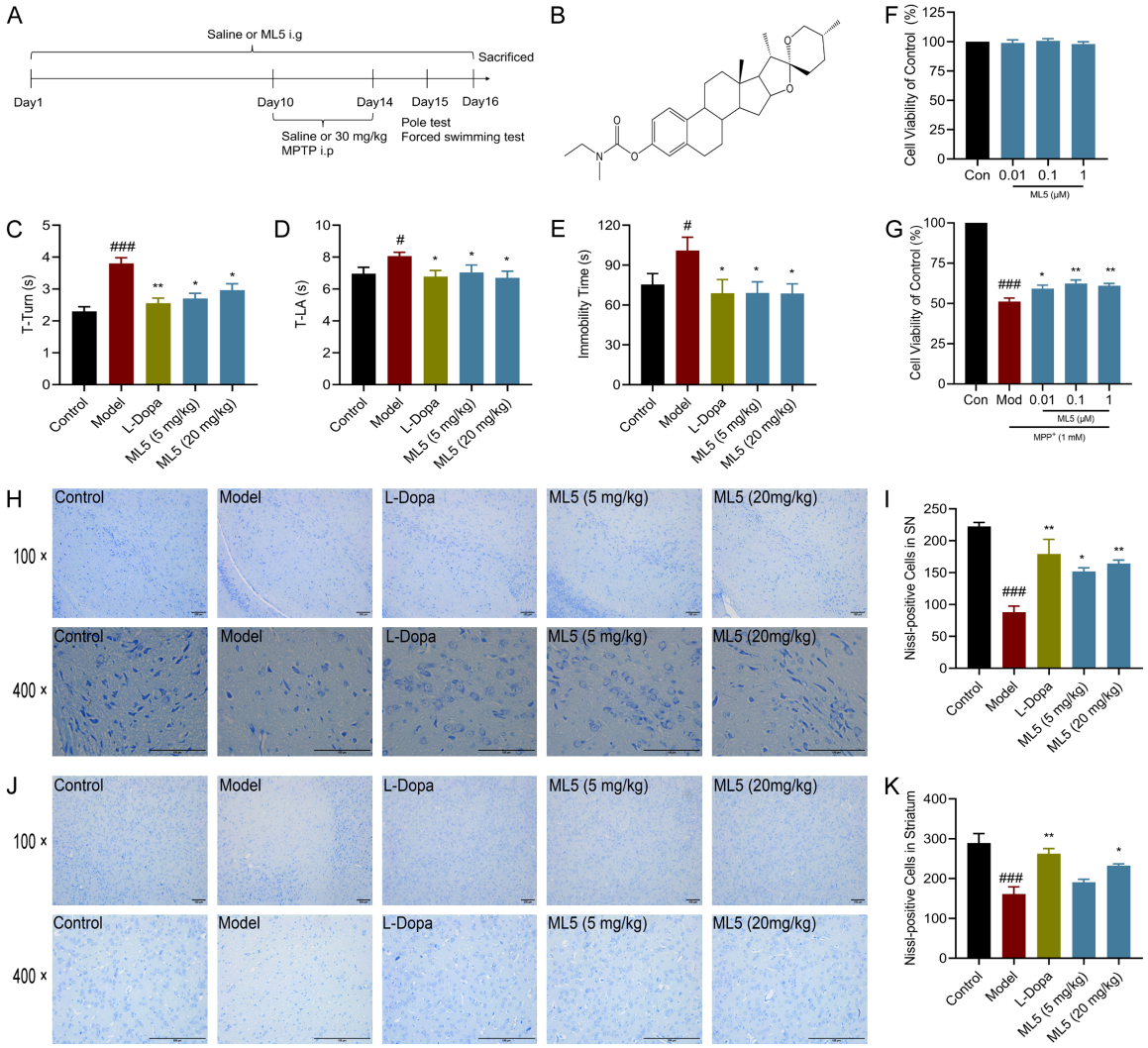

Figure 1. ML5 improved the pole test and forced swimming test in MPTP-treated mouse models of PD. (A) Experimental protocol of mouse models of PD. (B) Structure of compound ML5. (C, D) The graph showed the time used by mice to turn completely and climb down the pole. (E) Time during which mice remained immobile during the last 4 min. (F) SH-SY5Y cells were treated with ML5 for 24 h. (G) SH-SY5Y cells were treated with ML5 (0.01, 0.1, and 1 μM) for 2 h before being exposed to MPP^+ (1 mM) for 24 h. (H-K) Typical images of Nissl staining and quantification of Nissl-positive cells in the regions of SN and striatum (the magnified areas of the above images were shown in the lower images; both of the scale bars represented 100 μm). n = 10 in (C-E) n = 6 in (F and G), and n = 4 in (H-K). # and ### represented the *p*-values less than 0.05 and 0.001 compared to the control group; * and ** represented the *p*-values less than 0.05 and 0.01 compared to the model group.

Neurons in SN transport dopamine to the striatum through the SN-striatum circuit [21]. TH immunohistochemical staining of the striatum was similar to that of the SN. A densely arranged TH nerve fibers in the striatum and brown color were observed in the control group. In the model group, TH nerve fibers were sparse with a rather light color (**Figure 2C**). Statistical analysis also showed that TH nerve fibers' density in the striatum of the model group was drastically decreased. However, this decrease was dramatically improved by L-Dopa, as well as 5 mg/kg and 20 mg/kg ML5 administration (**Figure 2D**). The immunohistochemical staining analysis demonstrated that the model group showed a considerably reduced ChAT expression compared to the control group. Notably, obvious restoration of ChAT expression in the striatum was discovered in the three treated groups (**Figure 2E** and **2F**).

ML5 improved the levels of dopamine in the striatum of PD mice: With the loss of TH neurons, we observed a decreased striatal dopa-

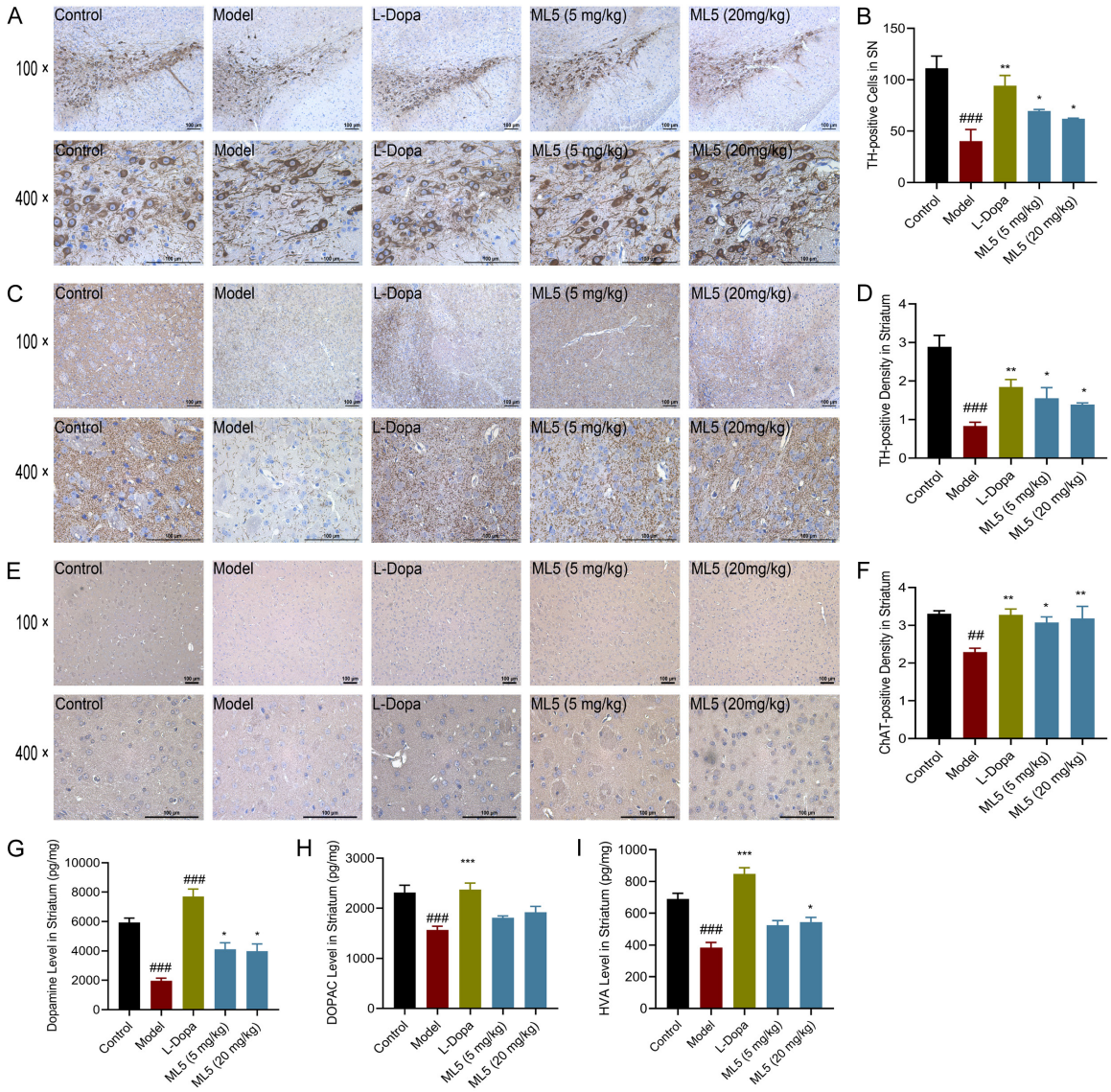

Figure 2. ML5 protected against damage of TH neurons in MPTP-induced mouse models of PD. (A, B) Representative images of TH staining and quantification of TH^+ cells in SN regions from PD mice (the magnified areas of the above images were shown in the lower images; both of the scale bars represented 100 μm). (C-F) Representative images of TH and ChAT staining and quantification of positive density in the striatum regions from PD mice (the magnified areas of the above images were shown in the lower images; both of the scale bars represented 100 μm). (G-I) The concentrations of dopamine, DOPAC, and HVA in the striatum of mice. n = 3 in (A-F), and n = 4 in (G-I). ## and ### represented the *p*-values less than 0.01 and 0.001 compared to the control group; *, **, and *** represented the *p*-values less than 0.05, 0.01, and 0.001 compared to the model group.

mine and its metabolites. An almost 70% decrease of dopamine was discovered in the MPTP-damaged model group. Of note, a reduction of only 40-50% was observed after treatment with 20 mg/kg of ML5 (**Figure 2G**). Furthermore, the concentrations of DOPAC and HVA in the striatum of the model group were also decreased. In contrast, these levels increased after treatment with L-Dopa and ML5 (**Figure 2H** and **2I**).

ML5 alleviated mitochondrial dysfunctions and protected mitochondrial morphology and the number of MPP^+-induced SH-SY5Y cells

ML5 increased the contents of ATP and MMP and reduced oxidative stress in MPP^+-induced SH-SY5Y cells: To supply energy for cellular life processes, mitochondria synthesize ATP through oxidative phosphorylation and the dysfunction of mitochondria could lead to de-

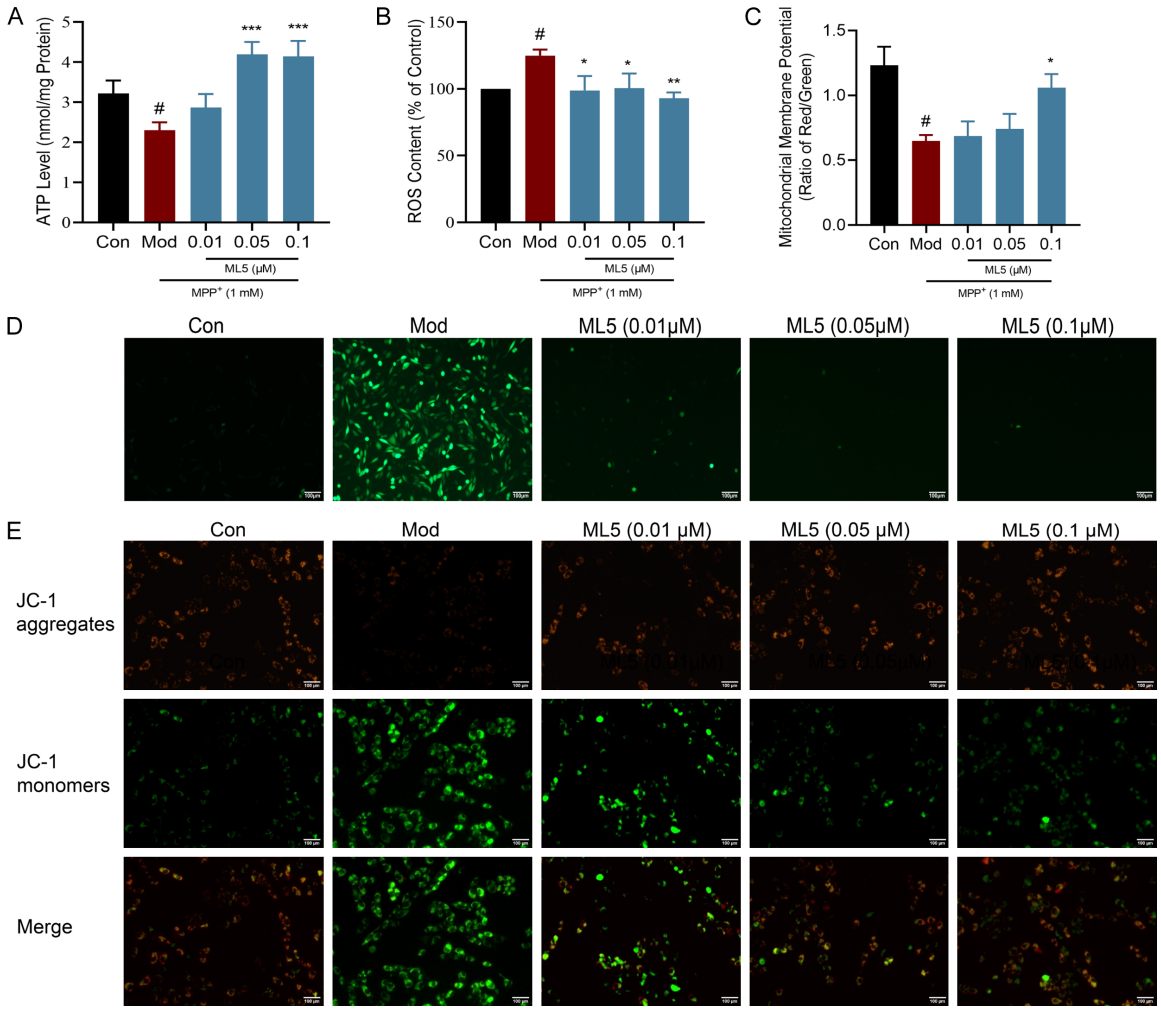

Figure 3. ML5 protected cell viability, ATP, ROS, and MMP levels in SH-SY5Y cells from MPP^+-induced damage. (A) ATP product detected using a bioluminescence assay kit. (B) Relative ROS levels measured through flow cytometry. (C) MMP was determined by a JC-1 detection kit. (D, E) Representative ROS and MMP images were captured by a fluorescence microscope (the scale bar represented 100 μm). n = 6 in (A-E). # represented the *p*-value less than 0.05 representatively compared to the control group; *, **, and *** represented the *p*-values less than 0.05, 0.01, and 0.001 compared to the model group.

creased ATP production [22]. As shown in **Figure 3A**, MPP^+-stimulated SH-SY5Y cells had significantly lower ATP levels than control cells. In contrast, ATP levels were significantly higher in cells treated with ML5 versus control cells treated with MPP^+ alone; statistically significant differences were observed after treatment with 0.05 μM and 0.1 μM ML5.

A considerably elevated ROS content in the model group was observed in comparison to the non-treated cells (**Figure 3B**). Similarly, the model group had a greater fluorescence value than the control group (**Figure 3D**). Never-theless, treatment with ML5 (0.01, 0.05, and 0.1 μM) effectively alleviated the excessive oxidative stress induced by MPP^+.

JC-1 is commonly used to measure MMP, which is indicated by red fluorescence/green fluorescence. As shown in **Figure 3C** and **3E**, there was a significant loss of MMP in cells treated with MPP^+ (1 mM). However, the MMP levels were elevated in cells treated with ML5 (0.1 μM) versus SH-SY5Y cells treated with MPP^+ alone. These results suggested that ML5 protected the MMP and oxidative phosphorylation in MPP^+-induced cells while reducing oxidative stress.

ML5 protected morphology and number of mitochondria in SH-SY5Y cells after MPP⁺ stimulation: As indicated in **Figure 4A**, mitochondria in the control cells had complete and longline shapes and were densely arranged and distributed around the nucleus. Nevertheless, in the cells of the model group, the mitochondria were separated and sparsely arranged. In comparison to the control group, the model group showed markedly low form factor (**Figure 4B**), indicating more fragmented mitochondria in the MPP⁺-stimulated cells. In addition, dramatically reduced average mitochondrial number was discovered in the model group compared to the non-treated control cells (**Figure 4C**). Nevertheless, the reduced number of mitochondria was partially restored by ML5 administration with different doses.

Next, the mitochondrial morphology of SH-SY5Y cells was further investigated through TEM. As shown in **Figure 4D**, compared with control, the MPP⁺-treated mitochondria were divided into smaller mitochondria; some mitochondria showed pathological morphologies, such as incomplete membrane, enlarged gap, and swollen volume. Nevertheless, this pathological condition was significantly improved after treatment with ML5. Mitochondrial stereology was used to analyze mitochondrial number density, mitochondrial surface density, and mitochondrial volume density. The findings confirmed that ML5 preserved the mitochondrial morphology and network, and delayed mitochondrial fission (**Figure 4E-G**). These results suggested that ML5 protected mitochondrial network morphology from the stimulation of MPP⁺.

ML5 mediated the biogenesis of mitochondria through enhancing AMPK/PGC-1α activation and regulated the fusion and fission of mitochondria

ML5 mediated mitochondrial biogenesis by activating the AMPK/PGC-1α signaling pathway: The above experiments demonstrated that ML5 promoted the recovery of mitochondrial function and morphology. Additionally, the regulatory effect of AMPK pathway on the biogenesis of mitochondria was also observed previously [23]. Thus, we explored the signaling pathways connected to the neuroprotective impact of ML5 in MPP⁺-induced SH-SY5Y cells. The results showed that treatment with MPP⁺ dramatically suppressed the phosphorylation of AMPK in SH-SY5Y cells (**Figure 5A**). In contrast to the model group, AMPK phosphorylation was upregulated in the ML5 (0.05 μM and 0.1 μM) treatment groups. This finding confirmed that treatment with ML5 activated the AMPK pathway in MPP⁺-stimulated cells. Activation of AMPK further regulated downstream signals SIRT1 and PGC-1α (**Figure 5B** and **5C**). SIRT1 and PGC-1α expressions were both considerably lower after treatment with MPP⁺ versus control; nevertheless, three doses of ML5 treatments significantly enhanced the impaired SIRT1 and PGC-1α expression by MPP⁺.

We have previously found [14] that ML5 promotes the translocation of NRF2 into the nucleus, while it is unclear whether ML5 affects the expression of total NRF2 and its target genes. Activation of the NRF2 pathway and induction of antioxidant enzymes triggered a protective mechanism against mitochondrial damage. A reduction of NRF2, TFAM, HO-1, and NQO-1 expression in MPP⁺-induced SH-SY5Y cells was found compared to the control cells. Nevertheless, this MPP⁺-induced reduction was significantly restored by ML5 administration, suggesting the regulatory effect of ML5 on the biogenesis of mitochondria through enhancing AMPK pathway activation (**Figure 5D-G**).

ML5 enhanced mitochondrial fusion and prevented mitochondrial fission: The expression of the molecules associated with the fission and fusion of mitochondria is regulated by the AMPK signaling pathway [24]. In mammals, Mfn1 and Mfn2 play a major role in mediating mitochondrial outer membrane fusion, while Opa1 plays a major role in mediating mitochondrial inner membrane fusion [25]. Additionally, Fis1 and Drp1 are significantly involved in the regulation of mitochondrial fission. Thus, we investigated the expression levels of these proteins using MPP⁺-induced SH-SY5Y cells. In comparison to the control, the model group exhibited significantly reduced Mfn1, Mfn2, and Opa1 expression, and elevated Fis1 and Drp1 expression. After treatment with ML5, the imbalance in mitochondrial fusion and fission was greatly reduced, as presented by an increase in Mfn1, Mfn2, and Opa1 expression, and a decrease in Drp1 and Fis1 expression

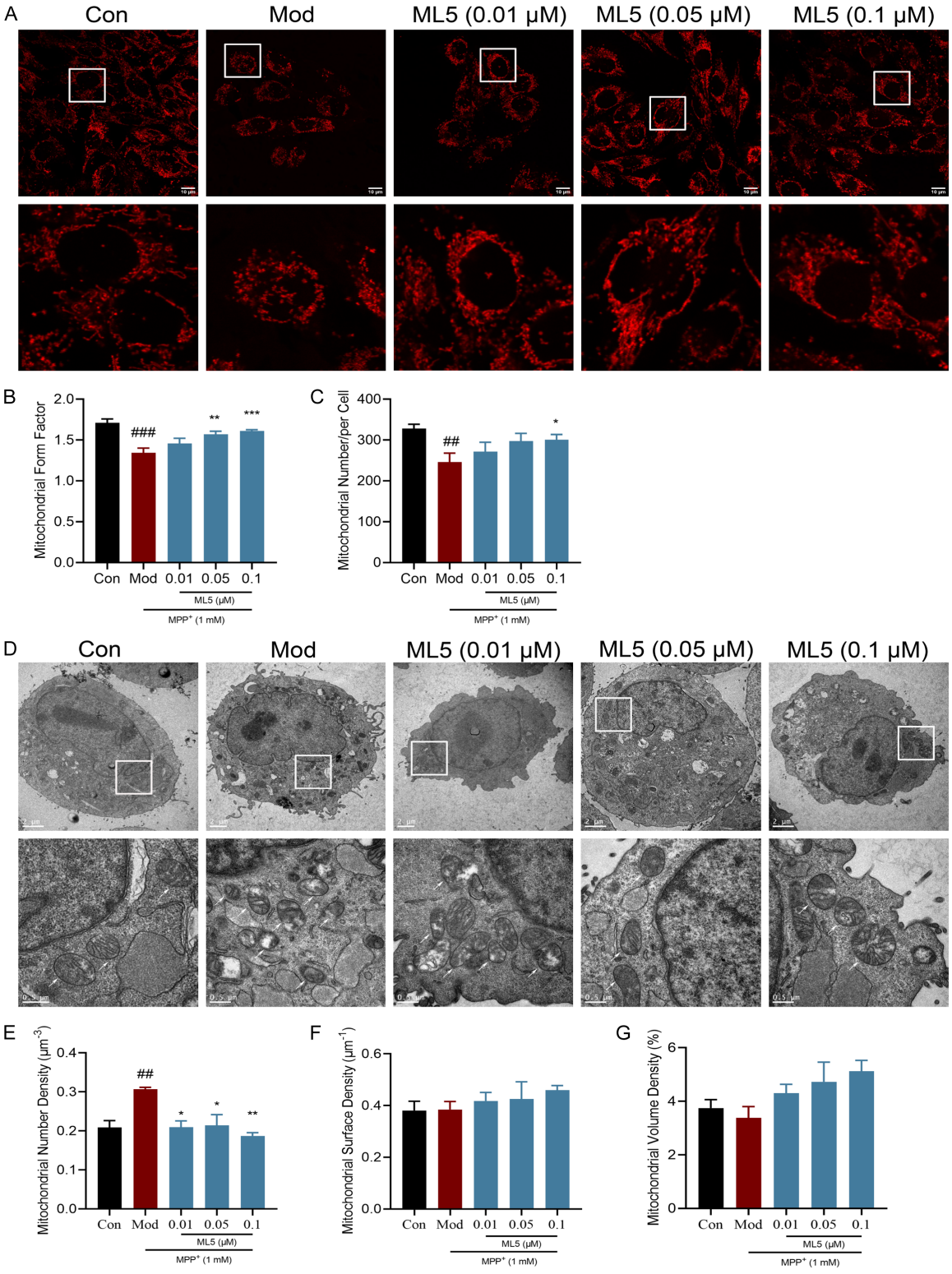

Figure 4. Effect of ML5 on mitochondrial morphology of cells with MPP⁺-induced damage. (A) The morphology of mitochondria in SH-SY5Y cells assessed using a confocal microscope (the magnified areas of the above images of the white boxes were shown in the lower images; the scale bars represented 10 μm). (B, C) Form factor and the number of mitochondria determined using the ImageJ software. (D) The morphology of mitochondria in SH-SY5Y cells assessed using a TEM (the magnified areas of the above images of the white boxes were shown in the lower images; the scale bars represented 2 μm and 0.5 μm respectively). (E) Mitochondrial number density, (F) mitochon-

drial surface density, and (G) mitochondrial volume density determined using the Image-Pro Plus 6.0 software. n = 4 in (A-C), and n = 3 in (D-G). ## and ### represented the *p*-values less than 0.01 and 0.001 compared to the control group; *, **, and *** represented the *p*-values less than 0.05, 0.01, and 0.001 compared to the model group.

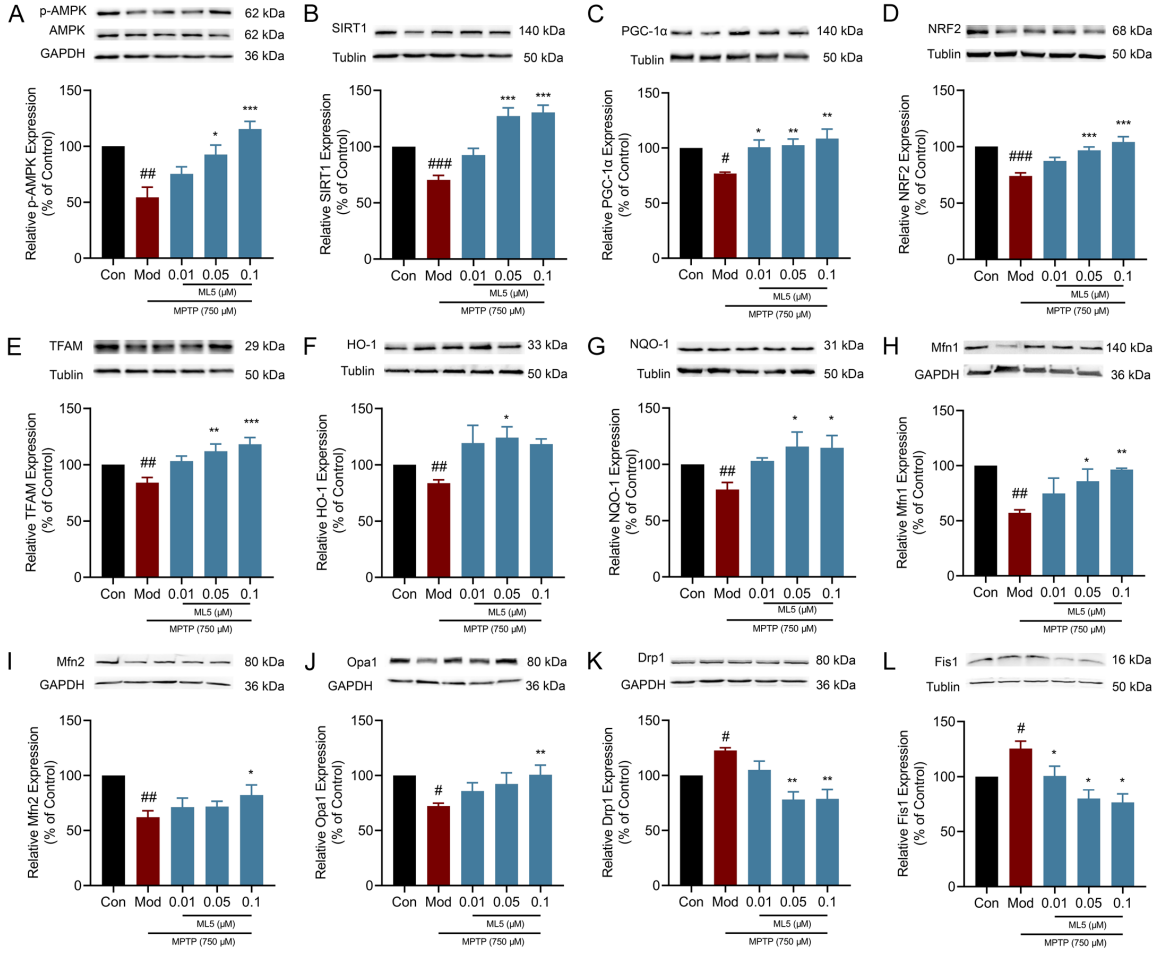

Figure 5. Impact of ML5 on the expression of AMPK signaling pathway and the proteins related to mitochondrial fusion/fission in cell models of PD. (A-C) Representative blots showing the expression of AMPK, SIRT1, and PGC-1α in SH-SY5Y cell models. (D-G) Representative blots showing the expression of NRF2, TFAM, HO-1, and NQO-1 in SH-SY5Y cell models. (H-L) Representative blots representing the expression of fusion-related proteins (Mfn1, Mfn2, and Opa1) and fission-related proteins (Drp1 and Fis1) in SH-SY5Y cells after pretreatment with ML5 and stimulation by MPTP. n = 3-6 in (A-L). #, ##, and ### represented the *p*-values less than 0.05, 0.01, and 0.001 compared to the control group; *, **, and *** represented the *p*-values less than 0.05, 0.01, and 0.001 compared to the model group.

(**Figure 5H-L**). These results demonstrated that ML5 might regulate the equilibrium between mitochondrial fusion and fission by activating the AMPK signaling pathway.

Neuroprotective effect of ML5 in MPP⁺-stimulated SH-SY5Y cells required activation of AMPK: As a potent and selective ATP-competitive AMPK inhibitor, dorsomorphin (compound C) is employed [26]. Dorsomorphin at different concentrations was used to induce injury to SH-SY5Y cells. We observed that dorsomorphin administration could dramatically impair cell viability, and the most pronounced effect was caused by 5 μM dorsomorphin (**Figure 6A**). Following the treatment of cells with dorsomorphin for 30 min, 2-hour protection of the cells with 0.1 μM ML5, and 24-hour damage with 1 mM MPP^+ were performed. The viability of cells was significantly decreased after exposure to MPTP compared with control, while treatment with 0.1 μM ML5 restored cell

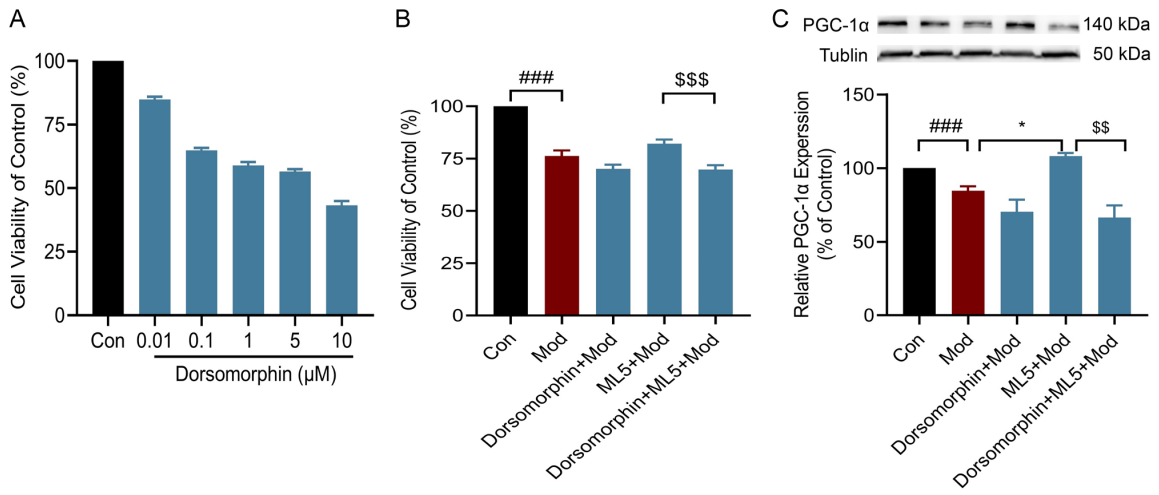

Figure 6. Preconditioning with the AMPK inhibitor dorsomorphin reversed the neuroprotective effect of ML5. (A) SH-SY5Y cells were treated with dorsomorphin for 24 h. (B) SH-SY5Y cells were treated with 5 μM dorsomorphin for 30 min; this was followed by the addition of 0.1 μM ML5 for 2 h and exposure to 750 μM MPTP for 24 h. (C) Representative blot representing PGC-1α expression was performed using the treatment method mentioned above. n = 6 in (A-C). ### represented the *p*-value less than 0.001 compared to the control group; * represented the *p*-value less than 0.05 compared to the model group; $$ and $$$ represented the *p*-values less than 0.01 and 0.001 compared to the ML5 treated group.

viability. Notably, preconditioning with dorsomorphin inhibited the efficacy of ML5 (**Figure 6B**).

In addition, western blotting analysis showed that treatment with MPTP drastically reduced PGC-1α expression. The expression of PGC-1α was elevated in 0.1 μM of ML5 treatment group compared with the model group, though the expression of PGC-1α was significantly inhibited by treatment with 5 μM dorsomorphin (**Figure 6C**).

Discussion

MPTP could be driven by mitochondrial membrane potential and diffuse into the mitochondria through the inner mitochondrial membranes. Studies showed that MPTP could inhibit the activity of not only complex I, but also complex III and IV [27]. MPTP could hinder the production of ATP, induce excessive ROS, and eventually lead to neuronal death. Moreover, MPTP could induce autonomic dysfunction *in vivo*, with decreased TH activity, and severely depleted dopamine levels in the striatum, similar to the clinical symptoms and pathological changes of PD [28]. Therefore, MPTP could be used to build PD models *in vivo*.

Dyskinesia is the major clinical feature of PD. The pole test can be used to reflect the motor coordination and agility in mice [29]. Therefore, it is highly sensitive to dysfunction of the SN and striatum. In this study, we observed that in comparison to the control group, the model group showed dramatically prolonged turning time and total time, demonstrating that MPTP damaged the motor coordination of mice. Treatment with low and high-dose ML5 exerted a similar therapeutic effect to that of L-Dopa. Depression is the main non-motor symptom of PD, affecting nearly 40% of patients with PD [30]. The forced swimming test directly reflects the depressive symptoms and, to a certain extent, the motor ability of mice with PD [31]. Our results revealed that compared to the control mice, PD mice needed more time for immobility, suggesting that MPTP successfully induced depressive symptoms in mice. Additionally, the forced swimming test of PD mice was significantly improved by ML5 either a low or a high dose, and the effect was similar to that exerted by treatment with L-Dopa. This result showed that ML5 could alleviate the depression of mice with PD and confirmed the results of the pole test.

The survival and level of dopaminergic neurons in the SN and striatum were detected using Nissl and immunohistochemistry staining. Similar to previously reported results [32], the present data showed that mice in the model

group lost >60% of the SN and striatum dopamine neurons, implying that MPTP successfully induced the pathological characteristics of PD in mice. Sconce et al. [33] reported that extensive dopamine loss was associated with a decline in movement ability, which was also consistent with the evidence obtained through behavioral tests. Treatment with ML5 could significantly alleviate these symptoms, reaching approximately 70% of the effect exerted by the positive drug L-Dopa.

Although the single neurotransmitter loss is considered as the pathogenesis of PD, this type of loss can affect other neurotransmitter systems. The degeneration of SN in PD can lead to increased cholinergic tone in the striatum, thereby impairing the nerve transmission of basal ganglia, and leading to motor symptoms in patients with PD [34]. ChAT is a marker enzyme for cholinergic neurons. In this study, dramatically reduced ChAT expression was observed in the striatum after MPTP stimulation, suggesting that the mechanism of MPTP-induced PD might include its effect on the cholinergic system. Our results were consistent with those previously reported by Hilario, et al. [35] and Pienaar, et al. [36]. Moreover, autopsy also showed obviously reduced ChAT expression in PD patients [37]. Treatment with ML5 could significantly reverse the damage induced by MPTP to the cholinergic system in the striatum. Combined with the immunohistochemical results of TH, ML5 could simultaneously regulate both dopaminergic and cholinergic disorders in the SN and striatum, facilitating the restoration of the balance between dopamine and acetylcholine levels and exerting a therapeutic effect against PD.

In dopaminergic neurons, tyrosine is catalyzed to L-Dopa by TH, which is subsequently decarboxylated by aromatic amino acid decarboxylase to produce dopamine. Dopamine is further catalyzed by monoamine oxidase to produce 3, 4-dihydroxyphenylacetaldehyde which, in the presence of aldehyde dehydrogenase, produces DOPAC. Thereafter, DOPAC can be converted to HVA by catechol-O-methyl transferase methylation [38]. Our results demonstrated that the levels of dopamine, DOPAC, and HVA were decreased by MPTP induction, and these changes were partially prevented after treatment with L-Dopa and ML5, suggesting that ML5 protects dopaminergic neurons from injury.

Normal mitochondrial activity is essential for the survival of neurons. The dysfunction of mitochondria is significantly connected to the early symptoms of numerous neurodegenerative disorders. Clinical studies have shown that the activity of complex I was dropped by 30-40% in the SN of patients with PD, and various therapies targeting mitochondrial dysfunction have exerted protective effects on animal models of PD [39]. We detected the concentration of ATP, ROS, and MMP to determine whether the protective impact of ML5 on PD cell models was related to the repair of mitochondrial dysfunction. Destruction of the mitochondrial respiratory chain affects mitochondrial respiratory function and reduces ATP production, which in turn causes electron leakage and ROS accumulation. Excessive production of ROS damages the mitochondrial respiratory chain, thus creating a vicious circle. MMP is a prerequisite for mitochondrial oxidative phosphorylation; its absence causes an imbalance in Ca^{2+} homeostasis, further damaging the activity of mitochondrial respiratory chain enzymes [40]. Our results indicated that ROS levels were elevated, whereas those of ATP and MMP were decreased in cell models of PD. Treatment with ML5 restored the levels of these three indicators of mitochondrial function, suggesting that ML5 could protect mitochondrial functions in this setting.

Eukaryotic cells maintain a normal shape and a certain number of mitochondria by balancing mitochondrial fusion and fission. Mitochondrial dynamics affect mitochondrial morphology and the physiological functions of mitochondria, such as the maintenance of Ca^{2+} homeostasis, ATP production, ROS level, and apoptosis. Evidence showed [41] that abnormal mitochondrial morphology preceded mitochondrial dysfunction. Therefore, the mitochondrial morphology of PD cell models was observed and analyzed to explore whether the role of ML5 in protecting mitochondrial function was related to mitochondrial dynamics. The results revealed that mitochondria in PD cell models were severely fragmented and tended to divide excessively, which was consistent with previous results reported in the literature [42]. Treatment with ML5 increased the length of mitochondria

and alleviated the degree of fragmentation, indicating that ML5 could help maintain the normal shape of mitochondria.

As a complex composed of α, β, and γ subunits, AMPK can activate PGC-1α by regulating the NAD^+/NADH ratios to activate SIRT1, which induces mitochondrial biogenesis [43]. PGC-1α significantly participates in the promotion of mitochondrial genes expression through coordinating with the nuclear hormone receptors and activating kinds of transcriptional factors. Research has demonstrated that PGC-1α could enhance the biogenesis of mitochondria through activating NRF2 transcription and increasing TFAM expression [44]. To confirm whether mitochondrial fragmentation was related to mitochondrial biogenesis in PD cell models, we measured AMPK and its downstream molecules expression. Our findings demonstrated that AMPK, SIRT1, PGC-1α, NRF2, and their downstream protein expression was remarkably suppressed after stimulation of MPTP. Importantly, protection with ML5 restored the levels of these proteins. The above results implied that ML5 could enhance the biogenesis of mitochondria through enhancing AMPK/PGC-1α expression, thereby restoring mitochondrial morphology and function.

Subsequently, we analyzed Mfn1, Mfn2, Opa1, Drp1, and Fis1 expression to elucidate the molecular mechanism by which ML5 affected mitochondrial fusion and fission. We observed that MPP^+ treatment could significantly reduce mitochondrial fusion-associated factors expression, such as Mfn1, Opa1, and Mfn2. In contrast, the protein levels of Drp1 and Fis1, which regulate mitochondrial fission, were elevated by MPP^+. These findings implied that the mitochondrial fusion activity was decreased and the fission activity was increased in the MPTP-induced model group. Combined with the experimental results of mitochondrial functional indicators, the results of our study supported the conclusions of previous research [45] reporting that decreased Mfn2 levels led to decreased ATP synthesis, Drp1 overexpression, and oxidative stress. In contrast, ML5 successfully reversed the aberrant expression of these five proteins, which was consistent with our observations in morphological experiments. These results suggested that ML5 could restore the unbalance between mitochondrial fusion and fission by promoting fusion and inhibiting fission of mitochondria to maintain normal mitochondrial morphology.

Moreover, Guo, et al. [46] reported that the overexpression of PGC-1α induced by high glucose levels led to reduced phosphorylation of Drp1 and improved mitochondrial fragmentation. In our experiments, we also demonstrated that PGC-1α expression was upregulated and the expression of Drp1 was down-regulated after protection with ML5. Therefore, we speculated that through promoting PGC-1α expression, ML5 could effectively balance the fission and fusion of mitochondria. To further prove the involvement of AMPK, we used the AMPK inhibitor dorsomorphin to restrain the AMPK-mediated activation of PGC-1α. The results showed that pretreatment with dorsomorphin reduced the viability of cells and PGC-1α expression after protection with ML5, indicating that PGC-1α was regulated by AMPK. Therefore, ML5 exerted neuroprotective effects by enhancing AMPK/PGC-1α pathway activation (**Figure 7**).

Conclusion

Collectively, our results suggest that ML5 can mediate PGC-1α expression through promoting AMPK pathway activation and balancing mitochondrial biogenesis and fusion/fission, thus restoring the function of mitochondria in cellular models. Furthermore, ML5 ameliorates MPTP-induced motor dysfunction and alleviates dopaminergic neuronal degeneration in mouse models of PD, thereby exerting a neuroprotective effect. These findings may shed a light on the underlying mechanisms of the course of PD and assist in the development of potentially therapeutic drugs.

Acknowledgements

This work was supported by the National Natural Science Foundation of China (Grant 81973196), the Natural Science Foundation of Shanghai, China (Grant 19ZR1413900) and the Joint Institute of Tobacco and Health, No. 367 Hongjin Road, Wuhua District, Kunming 650202,Yunnan,China(2022539200340111).

Disclosure of conflict of interest

None.

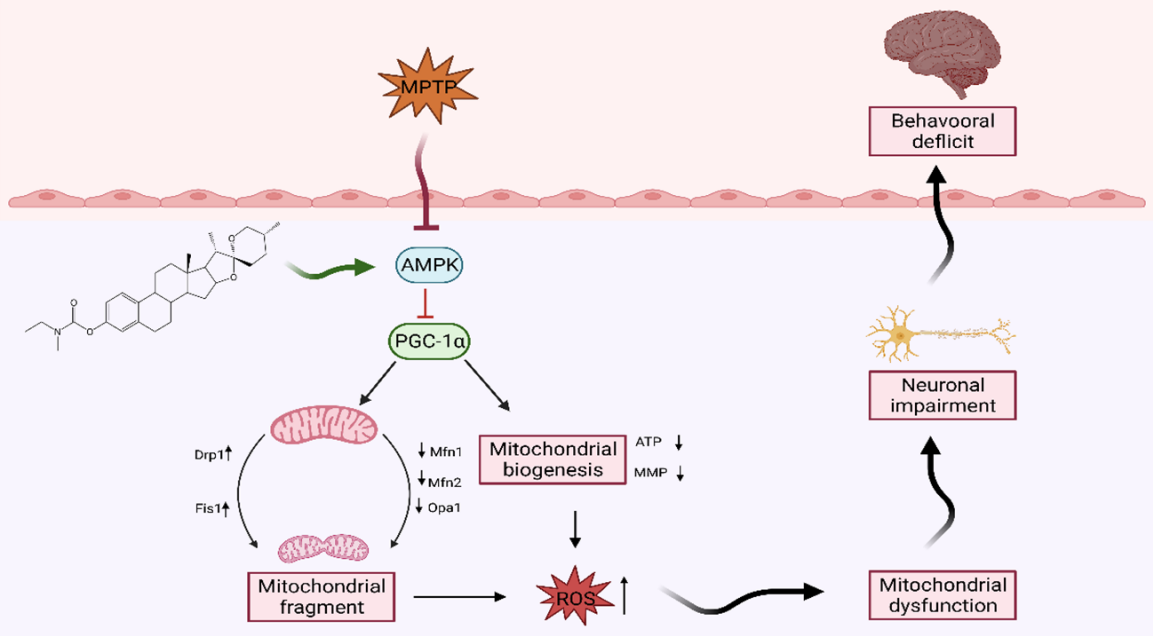

Figure 7. Protective function of ML5 on Parkinson's disease and possible underlying mechanisms. MPTP inhibited the production of ATP and MMP, induced an excessive production of ROS and excessive mitochondrial fission, caused mitochondrial dysfunction, and eventually led to neuronal death *in vitro*. MPTP also crossed the blood-brain barrier, thereby causing damage to dopaminergic neurons *in vivo*. ML5 prevented dopaminergic neurodegeneration and restored mitochondrial dysfunction by activating the AMPK/PGC-1α signaling pathway.

Address correspondence to: Drs. Rui Wang and Lei Ma, Shanghai Key Laboratory of New Drug Design, School of Pharmacy, East China University of Science and Technology, Shanghai 200237, China. E-mail: ruiwang@ecust.edu.cn (RW); malei@ecust.edu.cn (LM)

References

[1] Kehagia AA. Neuropsychiatric symptoms in Parkinson's disease: beyond complications. Front Psychiatry 2016; 7: 110.

[2] Schapira AH, Olanow CW, Greenamyre JT and Bezard E. Slowing of neurodegeneration in Parkinson's disease and Huntington's disease: future therapeutic perspectives. Lancet 2014; 384: 545-555.

[3] Gao J, Wang L, Liu J, Xie F, Su B and Wang X. Abnormalities of mitochondrial dynamics in neurodegenerative diseases. Antioxidants (Basel) 2017; 6: 25.

[4] Tubert C and Murer MG. What's wrong with the striatal cholinergic interneurons in Parkinson's disease? Focus on intrinsic excitability. Eur J Neurosci 2021; 53: 2100-2116.

[5] Peng K, Yang L, Wang J, Ye F, Dan G, Zhao Y, Cai Y, Cui Z, Ao L, Liu J, Zou Z, Sai Y and Cao J. The interaction of mitochondrial biogenesis and fission/fusion mediated by PGC-1α regulates rotenone-induced dopaminergic neurotoxicity. Mol Neurobiol 2017; 54: 3783-3797.

[6] Cantó C and Auwerx J. AMP-activated protein kinase and its downstream transcriptional pathways. Cell Mol Life Sci 2010; 67: 3407-3423.

[7] Chen Y, Jiang Y, Yang Y, Huang X and Sun C. SIRT1 protects dopaminergic neurons in Parkinson's disease models via PGC-1α-mediated mitochondrial biogenesis. Neurotox Res 2021; 39: 1393-1404.

[8] Cantó C and Auwerx J. PGC-1alpha, SIRT1 and AMPK, an energy sensing network that controls energy expenditure. Curr Opin Lipidol 2009; 20: 98-105.

[9] Golpich M, Amini E, Mohamed Z, Azman Ali R, Mohamed Ibrahim N and Ahmadiani A. Mitochondrial dysfunction and biogenesis in neurodegenerative diseases: pathogenesis and treatment. CNS Neurosci Ther 2017; 23: 5-22.

[10] Ding M, Feng N, Tang D, Feng J, Li Z, Jia M, Liu Z, Gu X, Wang Y, Fu F and Pei J. Melatonin prevents Drp1-mediated mitochondrial fission in diabetic hearts through SIRT1-PGC1α pathway. J Pineal Res 2018; 65: e12491.

[11] Cai B, Zhang Y, Wang Z, Xu D, Jia Y, Guan Y, Liao A, Liu G, Chun C and Li J. Therapeutic potential of diosgenin and its major derivatives against neurological diseases: recent advanc-

es. Oxid Med Cell Longev 2020; 2020: 3153082.
[12] Chojnacki JE, Liu K, Saathoff JM and Zhang S. Bivalent ligands incorporating curcumin and diosgenin as multifunctional compounds against Alzheimer's disease. Bioorg Med Chem 2015; 23: 7324-7331.
[13] Li B, Xu P, Wu S, Jiang Z, Huang Z, Li Q and Chen D. Diosgenin attenuates lipopolysaccharide-induced Parkinson's disease by inhibiting the TLR/NF-κB pathway. J Alzheimers Dis 2018; 64: 943-955.
[14] Yang GX, Sun JM, Zheng LL, Zhang L, Li J, Gan HX, Huang Y, Huang J, Diao XX, Tang Y, Wang R and Ma L. Twin drug design, synthesis and evaluation of diosgenin derivatives as multitargeted agents for the treatment of vascular dementia. Bioorg Med Chem 2021; 37: 116109.
[15] Xu YD, Cui C, Sun MF, Zhu YL, Chu M, Shi YW, Lin SL, Yang XS and Shen YQ. Neuroprotective effects of loganin on MPTP-induced Parkinson's disease mice: neurochemistry, glial reaction and autophagy studies. J Cell Biochem 2017; 118: 3495-3510.
[16] Ding GZ, Zhao WE, Li X, Gong QL and Lu Y. A comparative study of mitochondrial ultrastructure in melanocytes from perilesional vitiligo skin and perilesional halo nevi skin. Arch Dermatol Res 2015; 307: 281-289.
[17] Geng J, Liu W, Gao J, Jiang C, Fan T, Sun Y, Qin ZH, Xu Q, Guo W and Gao J. Andrographolide alleviates Parkinsonism in MPTP-PD mice via targeting mitochondrial fission mediated by dynamin-related protein 1. Br J Pharmacol 2019; 176: 4574-4591.
[18] Liang Y, Liu D, Ochs T, Tang C, Chen S, Zhang S, Geng B, Jin H and Du J. Endogenous sulfur dioxide protects against isoproterenol-induced myocardial injury and increases myocardial antioxidant capacity in rats. Lab Invest 2011; 91: 12-23.
[19] Asakawa T, Fang H, Sugiyama K, Nozaki T, Hong Z, Yang Y, Hua F, Ding G, Chao D, Fenoy AJ, Villarreal SJ, Onoe H, Suzuki K, Mori N, Namba H and Xia Y. Animal behavioral assessments in current research of Parkinson's disease. Neurosci Biobehav Rev 2016; 65: 63-94.
[20] Khan W, Priyadarshini M, Zakai HA, Kamal MA and Alam Q. A brief overview of tyrosine hydroxylase and α-synuclein in the Parkinsonian brain. CNS Neurol Disord Drug Targets 2012; 11: 456-462.
[21] Mandal S, Mandal SD, Chuttani K, Sawant KK and Subudhi BB. Design and evaluation of mucoadhesive microemulsion for neuroprotective effect of ibuprofen following intranasal route in the MPTP mice model. Drug Dev Ind Pharm 2016; 42: 1340-1350.
[22] Manevski M, Muthumalage T, Devadoss D, Sundar IK, Wang Q, Singh KP, Unwalla HJ, Chand HS and Rahman I. Cellular stress responses and dysfunctional Mitochondrial-cellular senescence, and therapeutics in chronic respiratory diseases. Redox Biol 2020; 33: 101443.
[23] Dite TA, Ling NXY, Scott JW, Hoque A, Galic S, Parker BL, Ngoei KRW, Langendorf CG, O'Brien MT, Kundu M, Viollet B, Steinberg GR, Sakamoto K, Kemp BE and Oakhill JS. The autophagy initiator ULK1 sensitizes AMPK to allosteric drugs. Nat Commun 2017; 8: 571.
[24] Yang J, Suo H and Song J. Protective role of mitoquinone against impaired mitochondrial homeostasis in metabolic syndrome. Crit Rev Food Sci Nutr 2021; 61: 3857-3875.
[25] Chen H, Detmer SA, Ewald AJ, Griffin EE, Fraser SE and Chan DC. Mitofusins Mfn1 and Mfn2 coordinately regulate mitochondrial fusion and are essential for embryonic development. J Cell Biol 2003; 160: 189-200.
[26] Cheng Q, Chen J, Guo H, Lu JL, Zhou J, Guo XY, Shi Y, Zhang Y, Yu S, Zhang Q and Ding F. Pyrroloquinoline quinone promotes mitochondrial biogenesis in rotenone-induced Parkinson's disease model via AMPK activation. Acta Pharmacol Sin 2021; 42: 665-678.
[27] Mizuno Y, Sone N, Suzuki K and Saitoh T. Studies on the toxicity of 1-methyl-4-phenylpyridinium ion (MPP+) against mitochondria of mouse brain. J Neurol Sci 1988; 86: 97-110.
[28] Sundström E, Fredriksson A and Archer T. Chronic neurochemical and behavioral changes in MPTP-lesioned C57BL/6 mice: a model for Parkinson's disease. Brain Res 1990; 528: 181-188.
[29] Meredith GE and Kang UJ. Behavioral models of Parkinson's disease in rodents: a new look at an old problem. Mov Disord 2006; 21: 1595-1606.
[30] Huang YH, Chen JH, Loh EW, Chan L and Hong CT. The effect of monoamine oxidase-B inhibitors on the alleviation of depressive symptoms in Parkinson's disease: meta-analysis of randomized controlled trials. Ther Adv Psychopharmacol 2021; 11: 2045125320985993.
[31] Yamada K, Kobayashi M, Mori A, Jenner P and Kanda T. Antidepressant-like activity of the adenosine A(2A) receptor antagonist, istradefylline (KW-6002), in the forced swim test and the tail suspension test in rodents. Pharmacol Biochem Behav 2013; 114-115: 23-30.
[32] Duce JA, Wong BX, Durham H, Devedjian JC, Smith DP and Devos D. Post translational changes to α-synuclein control iron and dopamine trafficking; a concept for neuron vulnerability in Parkinson's disease. Mol Neurodegener 2017; 12: 45.

[33] Sconce MD, Churchill MJ, Greene RE and Meshul CK. Intervention with exercise restores motor deficits but not nigrostriatal loss in a progressive MPTP mouse model of Parkinson's disease. Neuroscience 2015; 299: 156-174.
[34] Hagino Y, Kasai S, Fujita M, Setogawa S, Yamaura H, Yanagihara D, Hashimoto M, Kobayashi K, Meltzer HY and Ikeda K. Involvement of cholinergic system in hyperactivity in dopamine-deficient mice. Neuropsychopharmacology 2015; 40: 1141-1150.
[35] Hilario WF, Herlinger AL, Areal LB, de Moraes LS, Ferreira TA, Andrade TE, Martins-Silva C and Pires RG. Cholinergic and dopaminergic alterations in nigrostriatal neurons are involved in environmental enrichment motor protection in a mouse model of Parkinson's disease. J Mol Neurosci 2016; 60: 453-464.
[36] Pienaar IS, Gartside SE, Sharma P, De Paola V, Gretenkord S, Withers D, Elson JL and Dexter DT. Pharmacogenetic stimulation of cholinergic pedunculopontine neurons reverses motor deficits in a rat model of Parkinson's disease. Mol Neurodegener 2015; 10: 47.
[37] Ruberg M, Ploska A, Javoy-Agid F and Agid Y. Muscarinic binding and choline acetyltransferase activity in Parkinsonian subjects with reference to dementia. Brain Res 1982; 232: 129-139.
[38] Wang XR, Zhu SX, Wen XM, Xie JX and Song N. Altered dopamine metabolism and its role in pathogenesis of Parkinson's disease. Sheng Li Xue Bao 2021; 73: 89-102.
[39] Beal MF. Mitochondria, oxidative damage, and inflammation in Parkinson's disease. Ann N Y Acad Sci 2003; 991: 120-131.
[40] Dou JP, Wu Q, Fu CH, Zhang DY, Yu J, Meng XW and Liang P. Amplified intracellular Ca(2+) for synergistic anti-tumor therapy of microwave ablation and chemotherapy. J Nanobiotechnology 2019; 17: 118.
[41] Xu S, Pi H, Zhang L, Zhang N, Li Y, Zhang H, Tang J, Li H, Feng M, Deng P, Guo P, Tian L, Xie J, He M, Lu Y, Zhong M, Zhang Y, Wang W, Reiter RJ, Yu Z and Zhou Z. Melatonin prevents abnormal mitochondrial dynamics resulting from the neurotoxicity of cadmium by blocking calcium-dependent translocation of Drp1 to the mitochondria. J Pineal Res 2016; 60: 291-302.
[42] Jiao Y, Zheng Y and Song CJ. Protective effect of edaravone on balance of mitochondrial fusion and fission in MPP(+)-treated PC12 cells. Sheng Li Xue Bao 2020; 72: 249-254.
[43] Gong Y, Wang C, Jiang Y, Zhang S, Feng S, Fu Y and Luo Y. Metformin inhibits tumor metastasis through suppressing Hsp90α secretion in an AMPKα1-PKCγ dependent manner. Cells 2020; 9: 144.
[44] Motlagh Scholle L, Schieffers H, Al-Robaiy S, Thaele A, Dehghani F, Lehmann Urban D and Zierz S. The effect of resveratrol on mitochondrial function in myoblasts of patients with the common m.3243A>G mutation. Biomolecules 2020; 10: 1103.
[45] Wang W, Zhang F, Li L, Tang F, Siedlak SL, Fujioka H, Liu Y, Su B, Pi Y and Wang X. MFN2 couples glutamate excitotoxicity and mitochondrial dysfunction in motor neurons. J Biol Chem 2015; 290: 168-182.
[46] Guo K, Lu J, Huang Y, Wu M, Zhang L, Yu H, Zhang M, Bao Y, He JC, Chen H and Jia W. Protective role of PGC-1α in diabetic nephropathy is associated with the inhibition of ROS through mitochondrial dynamic remodeling. PLoS One 2015; 10: e0125176.